

Flavopiridol Induces p53 via Initial Inhibition of Mdm2 and p21 and, Independently of p53, Sensitizes Apoptosis-Reluctant Cells to Tumor Necrosis Factor

Zoya N. Demidenko and Mikhail V. Blagosklonny

Brander Cancer Research Institute and Department of Medicine, New York Medical College, Valhalla, New York

ABSTRACT

Flavopiridol (FP) inhibits gene expression and causes apoptosis, and these effects cannot be explained by inhibition of cyclin-dependent kinases that govern cell cycle. The simple and established notion that FP is an inhibitor of transcription predicts its effects. Because Mdm-2 targets p53 for degradation, FP, as predicted, dramatically induced p53 by inhibiting Mdm-2. Once p53 was induced, restoration of transcription (by removal of FP) resulted in superinduction of p21 and Mdm-2. Similarly, low concentrations of FP (50 nM) induced p21 and Mdm-2 because of their initial down-regulation. A sustained decrease of Mdm-2/p21 expression and accumulation of p53 coincided with near-maximal cytotoxicity of FP at concentrations >100 nM. Induction of p53 was a marker, not a cause, of cytotoxicity. FP caused rapid apoptosis (caspase-dependent cell death) in p53-null leukemia cells. In these cells, FP-induced apoptosis was converted to growth arrest by inhibitors of caspases. In apoptosis-reluctant A549 and PC3M cancer cells, FP inhibited cell proliferation but did not cause apoptosis. Like typical inhibitors of transcription, FP sensitized cells to apoptotic stimuli, allowing tumor necrosis factor to cause rapid and massive apoptosis in otherwise apoptosis-reluctant cells. We discuss that, as a reversible inhibitor of transcription, FP can be used clinically in novel rational drug combinations.

INTRODUCTION

Cyclin-dependent kinases (cdks) are promising anticancer drug targets. Inhibitors of cdks are cytotoxic to cancer cells *in vitro* and suppress tumor growth in animals (1–4). Flavopiridol (FP), a pan-cdk inhibitor, is undergoing clinical trials either as a single agent or in combination with other agents, such as paclitaxel (5–8). By inhibiting cdk-4, -2, and -1, FP arrests cell cycle in G₁ and G₂ phases (9, 10). However, most effects of FP are neither consistent with inhibition of these cdks nor cell cycle specific. First, cdk-2 is dispensable for cancer cell growth, and mice lacking cdk-2 or cdk-4 develop normally (11–14). Therefore, it is not clear how FP causes G₁ arrest. Second, FP is a highly cytotoxic agent and induces apoptosis, a cell death mediated by caspases. There is no obvious reason why inhibition of cell cycle by FP should be extremely cytotoxic, and there is no satisfactory explanation why inhibition of cdks should cause apoptosis. Third, FP kills not only proliferating cells but also resting cells (15). Why should an inhibitor of cdks affect resting cells? Fourth, FP down-regulates multiple proteins such as cyclins D and B, vascular endothelial growth factor, X-linked inhibitor of apoptosis protein (XIAP), cIAP-2, Mcl-1, survivin, and p21 (16–22). Why does inhibition of cdks result in rapid down-regulation of these proteins, which either act upstream of cdks (cyclin D1, p21) or regulate apoptosis (Mcl-2, XIAP)? It was tempting to explain down-regulation of each protein by different mechanism. For example, it was suggested that FP-activated caspases cleave p21 (3), whereas FP-induced E2F inhibits

Mcl-1 expression (18). Fifth, FP induces p53 that is difficult to explain based on inhibition of cdks (23, 24).

In a largely unappreciated twist, FP turned out to be an inhibitor of transcription (24–28). FP inhibits cdk-9 (25, 29), which (in complex with cyclin T) is the transcriptional elongation factor P-TEFb, which does not participate in cell cycle regulation but is essential for transcription, controlling elongation by RNA polymerase II (30). FP inhibits transcriptional elongation *in vitro* by targeting cdk-9 at an IC₅₀ 5–10-fold lower than required for its effect on any other cdk (26). Similarly, 5,6-Dichloro-1-β-D-ribofuranosylbenzimidazole (DRB), a classic inhibitor of transcription, inhibits cdk-9, thus blocking transcription (31). FP changes gene expression profiles in an identical manner to the transcriptional inhibitor DRB (27). DRB could substitute for FP in drug combinations (32). In other words, mechanisms of action of FP and DRB are identical. In contrast, actinomycin D, an inhibitor of transcription and a DNA-damaging drug, inhibits initiation of transcription by intercalating into DNA.

The fact that FP blocks transcription can explain its puzzling effects. All of the proteins that are down-regulated by FP must have a short half-life for mRNA and protein (27). FP decreases XIAP, cIAP-2, Mcl-1, Bcl-xL, p21, Mdm-2, and survivin on mRNA levels (22, 33). It has been shown that FP, like other inhibitors of transcription, down-regulates thousands of mRNAs that have a short half-life (27). Furthermore, inhibition of transcription may result in “paradoxical” induction of certain proteins such as p53. Normally, p53 *trans*-activates Mdm-2, which in turn targets p53 for degradation. By inhibiting transcription of Mdm-2, actinomycin D and DRB prevent degradation of p53, thus inducing p53 (31, 34). Because FP is an inhibitor of transcription, a decrease in Mdm-2 expression then must precede and accompany induction of p53 caused by FP. (In contrast, following DNA damage, induction of p53 parallels induction of p21 and Mdm-2). It is firmly established that FP inhibits transcription and thus decreases expression of short-lived mRNAs, including Mdm-2 (22, 24–27, 33, 35). Yet, can inhibition of transcription be translated on protein levels to cause p53 induction and other effects of FP? We will investigate effects of FP on protein levels, including relationships between p53, Mdm-2, and p21.

Second, because FP is an inhibitor of transcription, we can predict that it will sensitize cancer cell to tumor necrosis factor (TNF). TNF activates caspases but transcriptionally induces inhibitors of caspases. By preventing TNF-induced transcription, actinomycin D permits apoptosis. Like actinomycin D, FP then must potentiate TNF-induced apoptosis. We tested these predictions and additionally investigated the relationship between cytotoxicity, p53 induction, and sensitization to apoptotic stimuli. On the basis of the assumption that inhibition of the same process (namely, transcription) is a single cause of all of the effects of FP, we expected that cytotoxicity (growth inhibition and apoptosis), p53 induction, and potentiation of TNF-induced apoptosis should correlate in a dose-dependent fashion.

MATERIALS AND METHODS

Cell Lines and Chemotherapeutic Agents. Human prostate cancer cell lines; LNCaP and PC3M cells; A549, a lung carcinoma cell line; and three

Received 1/23/04; revised 3/2/04; accepted 3/4/04.

The costs of publication of this article were defrayed in part by the payment of page charges. This article must therefore be hereby marked *advertisement* in accordance with 18 U.S.C. Section 1734 solely to indicate this fact.

Requests for reprints: Mikhail V. Blagosklonny, Brander Cancer Research Institute, 19 Bradhurst Avenue, Suite 2400, Hawthorne, NY 10532. Phone: 914-347-2801; Fax: 914-347-2804; E-mail: M_Blagosklonny@nycm.edu.

leukemia cell lines (HL60, Jurkat, and U937) were obtained from American Type Culture Collection (Manassas, VA). Human colon cancer cell line, HCT116, and clones lacking p21 or p53, p21^{-/-}, and p53^{-/-}, respectively, were a gift from Dr. B. Vogelstein (John Hopkins University, Baltimore, MD). All of the cell lines were maintained in RPMI 1640 medium and 10% fetal bovine serum. Adriamycin, actinomycin D, α -amanitin, and DRB were obtained from Sigma (St. Louis, MO). Adriamycin was dissolved in DMSO as a 2-mg/ml stock solution. Actinomycin D was dissolved in water as 2-mg/ml solutions. DRB was prepared as 100-mM stock solution. FP was obtained from the Development Therapeutics Program (National Cancer Institute, Bethesda, MD). FP was prepared as 10-mM stock solution in DMSO.

Transient Transfection. PG13-Luc, containing a generic p53 response element, was obtained from Dr. El-Deiry. The control luciferase plasmid, pGL2-control, driven by SV40 promoter and enhancer sequences, was purchased from Promega (Madison, WI). Fifty thousand cells were plated in 24-well plates (Costar, Acton, MA). The next day, cells were transfected with plasmids as described previously (36). After 6–16 h, the medium was changed, and cells were treated with FP for an additional 16 h. Cells were lysed and analyzed for luciferase activity (36).

Immunoblot Analysis. Cells were lysed, and soluble proteins were harvested in TNES buffer [50 mM TrisHCl (pH 7.5), 100 mM NaCl, 2 mM EDTA, 1 mM sodium orthovanadate, and 1% (v/v) NP40] containing protease inhibitors (20 μ g/ml aprotinin, 20 μ g/ml leupeptin, and 1 mM phenylmethylsulfonyl fluoride). Proteins were resolved with 7.5% SDS-PAGE for detection of Mdm-2, poly(ADP-ribose) polymerase (PARP), and p53 or with 12.5% SDS-PAGE for detection of p21, cyclin D1, and p53 as described previously (34, 36). Alternatively, proteins were resolved on NuPAGE 4–12% Bis-Tris gel with 4-morpholinepropanesulfonic acid running buffer (NOVEX, San Diego, CA) according to the manufacturer's instructions. Immunoblot analysis was performed using the following antibodies: monoclonal mouse antihuman p21 (EA10; Oncogene, Calbiochem, San Diego, CA), monoclonal mouse antihuman p53 (Ab2 and Ab6; Oncogene, Calbiochem), rabbit polyclonal antihuman cyclin D1 (H-295; Santa Cruz Biotechnology, Santa Cruz, CA), and rabbit polyclonal antihuman PARP (Upstate Biotechnology, Lake Placid, NY). Mdm-2 (Oncogene, Calbiochem), antihuman Raf-1, cyclin D1 polyclonal (C12; Santa Cruz Biotechnology), and antihuman Bcl-2 monoclonal (Dako, Glostrup, Denmark) antibodies were purchased, and mouse monoclonal antihuman tubulin antibodies were obtained from Sigma (St. Louis, MO). Immunoblots were developed using a horseradish peroxidase-conjugated secondary antibody (Bio-Rad, Hercules, CA) and a chemiluminescence detection kit (Dupont NEN, Boston, MA).

DNA Synthesis. DNA synthesis was monitored by [³H]thymidine incorporation as described previously (34). In brief, 25,000 cells were plated in 48-well flat-bottomed plates. The next day, cells were treated with drugs. At the indicated time, cells were incubated with 1 μ Ci [methyl³H]thymidine (Amersham, Piscataway, NJ), and acid-insoluble radioactivity then was determined.

Cell Cycle Analysis. Cells were harvested, washed with PBS, and resuspended in 75% ethanol in PBS and kept at 4°C for at least 30 min. Before analysis, cells were washed again with PBS and resuspended and incubated for 30 min in propidium iodide staining solution containing 0.05 mg/ml propidium iodide (Sigma) in PBS. The suspension then was passed through a nylon mesh filter and analyzed on a FACScan (Becton Dickinson, Franklin Lakes, NJ; Ref. 34).

MTT Assay. Two thousand cells were plated in 96-well flat-bottomed plates in 100 μ l of medium. The next day, cells were exposed to the pharmacologic agents. After 3 days of the last drug addition, 20 μ l of 5 mg/ml MTT solution in PBS were added to each well for 4 h. The medium was discarded, and 170 μ l DMSO were added to each well to dissolve the formazan crystals. The absorbance at 540 nm was determined using a Biokinetics plate reader (Bio-Tek Instruments, Inc, Winooski, VT). Triplicate wells were assayed for each condition, and SDs were determined.

Number of Dead and Live Cells. Twenty-five thousand cells were plated in 24-well plates in 1 ml of medium. The next day, cells were treated with the drugs. After 3–4 days, cells were trypsinized; each condition was counted with trypan blue; and the number of blue (dead) cells and transparent (live) cells was counted by microscopy.

DAPI Staining for Nuclear Fragmentation. Cells were with tested drugs for 12–16 h. Cells were subsequently trypsinized, washed with PBS, pelleted

onto glass slides in a cytocentrifuge, fixed with 90% ethanol/10% glacial acetic acid, and stained with 4',6-diamidino-2-phenylindole (DAPI; Molecular Probes, Eugene, OR) as described previously. Nuclei were visualized by UV microscopy.

RESULTS

Although Inhibiting Mdm-2 and p21, FP Induces Wild-Type p53 in HCT116 Cells. We demonstrated previously that by inhibiting transcription of Mdm-2 and p21, transcriptional inhibitors (actinomycin D, amanitin, and DRB) cause accumulation of p53 in HCT116, LNCaP, and A549 cells (34). We investigated effects of FP on Mdm-2, p21, and p53 (Fig. 1A). In addition, we measured cyclin D1, which is a p53-independent, short-lived protein. As shown in Fig. 1A, a brief exposure (4 h) to FP decreased Mdm-2 levels, with corresponding up-regulation of p53. At 25–50 nM FP, there was a rebound of Mdm-2 and p21 caused by spontaneous recovery by 16 h from transient effects of such low concentrations of FP, as we will discuss later. By 16 h, at ≥ 100 nM, FP down-regulated Mdm-2 and cyclin D1. At concentrations of 200 nM, FP down-regulated p21 (Fig. 1A). Simultaneously, 200–400 nM FP dramatically induced p53. Therefore, at 200–400 nM, FP inhibited all of the three proteins (p21, Mdm-2, and cyclin D1), whereas it induced p53. This corresponds to maximal cytotoxicity of FP (Fig. 1B). We conclude that FP inhibited Mdm-2 and p21 and reciprocally induced p53 at cytotoxic concentrations. These effects are ascribed to inhibition of transcription, which occurs at FP concentrations ≥ 100 nM (26, 27). Induction of p53 may serve as a marker inhibition of transcription by FP, in turn causing cytotoxicity.

Paradoxical p21 Induction at Subcytotoxic Doses of FP. At subcytotoxic concentrations (namely, 50–100 nM), FP caused seemingly unexpected effects. At 16 h, 100 nM FP induced p53 and p21 (Fig. 1A). We showed previously that subcytotoxic concentrations of DRB, a transcriptional inhibitor, coinduced p21, Mdm-2, and p53, consistent with spontaneous relief of transcriptional repression (34). Similarly, at low concentrations, either FP can be used up or cdk-9 can be replenished over time. It is expected that inhibition of transcription is transient at low concentrations of FP. During initial decrease in Mdm-2 (Fig. 1A; 4 h), p53 started its accumulation. This accumulated p53 is a potential driving force for induction of p21 and Mdm-2 (but not cyclin D1) by 16 h (100 nM FP), once transcription was restored. Therefore, we predict that only p53-dependent proteins should be superinduced at low concentrations of FP. In agreement, cyclin D1, which is not a p53-dependent protein, was decreased by 100 nM FP (Fig. 1A; 16 h). We conclude that 50–100 nM FP (subcytotoxic concentrations) inhibit transcription but cannot sustain this inhibition.

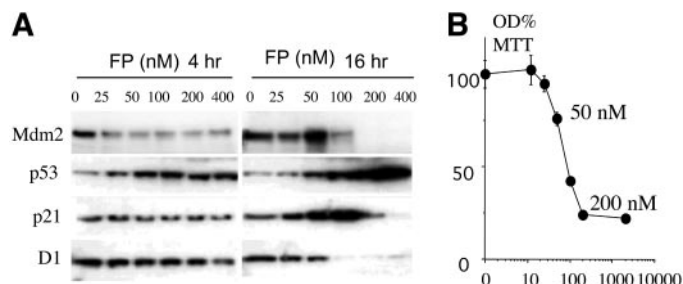


Fig. 1. Effects of flavopiridol (FP) on p53, p21, Mdm-2, and cyclin D1 (D1) and cytotoxicity. A, HCT116 cells were treated with indicated concentrations of flavopiridol (FP) for either 4 h or 16 h. Mdm-2, p53, p21, and D1 were determined by immunoblot analysis as described in "Materials and Methods." B, HCT116 cells were treated with indicated concentrations of FP. MTT assay was performed after 3 days as described in "Materials and Methods." Results were calculated as the percentage of values obtained with untreated cells and represent mean \pm SD.

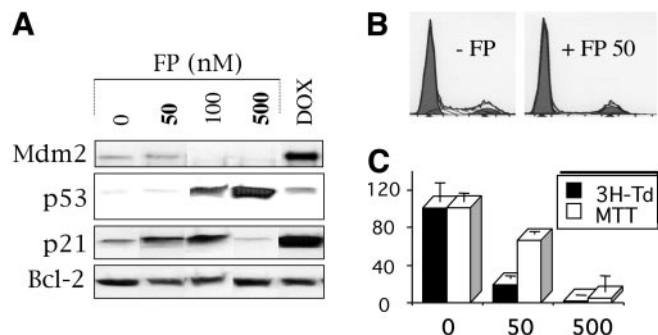


Fig. 2. Effects of low and high concentrations of flavopiridol (FP) on p53 and cell survival. **A**, LNCaP cells were treated with indicated concentrations of FP for 16 h. Cells were lysed, and Mdm-2, p53, p21, and Bcl-2 (for equal loading) were determined by immunoblot analysis. **B**, LNCaP cells were treated with 50 nM FP for 16 h. Flow cytometry was performed as described in "Materials and Methods." **C**, LNCaP cells were treated with the indicated concentrations of FP. After 16 h, [^3H]thymidine ($^3\text{H-Td}$) incorporation was measured as described in "Materials and Methods." In a parallel experiment, MTT assay was performed after 3 days. Results were calculated as the percentage of values obtained with untreated cells and represent mean \pm SD.

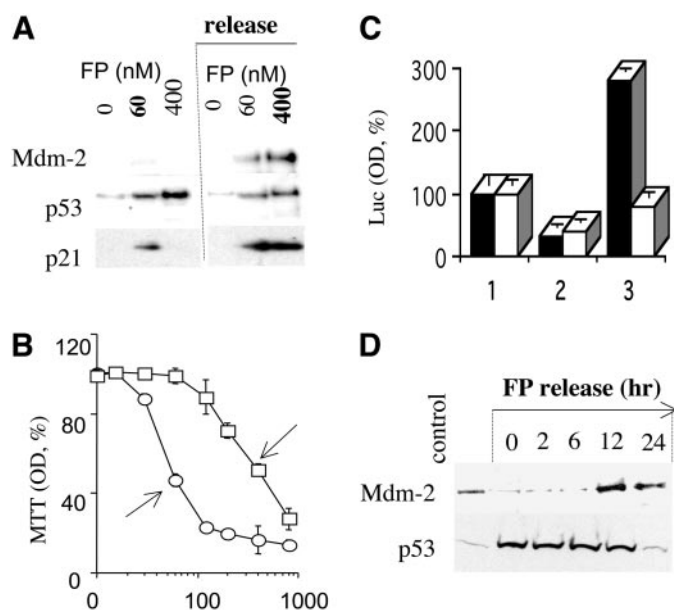


Fig. 3. Reversal of flavopiridol (FP) effects and rebound of p53-dependent transcription. **A**, LNCaP cells were treated with indicated concentrations of FP (left). After 16 h, the medium was changed for an additional 8 h (release). Mdm-2, p53, and p21 were measured by immunoblot analysis. **B**, LNCaP cells were treated with indicated concentrations of FP for 3 days (\circ), and MTT assay was performed as described in "Materials and Methods." In a parallel experiment, the medium was changed (\square) after 16 h. MTT assay (\circ) was performed after 3 days. Results were calculated as the percentage of values obtained with untreated cells and represent mean \pm SD. **C**, LNCaP cells were transfected with cytomegalovirus-Luc (open bars) and PG13-Luc (closed bars) as described in "Materials and Methods" and then treated with 400 nM FP for 16 h, treated with FP, and then the medium was changed for 8 h (release) or left untreated (control). The luciferase activity was measured as described in "Materials and Methods" and shown as percentage of control. **D**, a time course of p53 and Mdm-2 induction following removal of FP in A549 cells. A549 cells were treated with 500 nM FP for 16 h. The medium then was changed, and cells were cultured in the fresh medium for additional 0, 2, 6, 12, and 24 h. In control, cells were not treated with FP. Cells were lysed, and immunoblot analysis for Mdm-2 and p53 was performed as described in "Materials and Methods."

At doses ≥ 200 nM, FP was able to sustain the inhibition of transcription, corresponding to increased p53 and cytotoxicity.

We next extended these observations to LNCaP cells. At cytotoxic concentrations (e.g., 200–500 nM), FP down-regulated Mdm-2 and p21 and induced p53 (Fig. 2A). This is a hallmark of cytotoxic concentrations of FP: down-regulation of p21/Mdm2 with dramatic induction of p53. In comparison, the DNA-damaging drug doxorubicin induced p53, p21, and Mdm-2. By decreasing concentration of FP,

we were able to observe reappearance of p21, whereas Mdm-2 still was inhibited (Fig. 2A; 100 nM). This reflects the fact that p21 is more readily inducible by p53 and that Mdm-2 is more sensitive to transcription inhibition (37, 38). Therefore, at narrow range (100 nM), expression of p21 and Mdm-2 was dissociated. Finally, 50 nM FP induced p21 without detectable induction of p53, consistent with transient inhibition of transcription. Therefore, we evaluated effects of 50 nM FP on cell cycle and survival. Coincident with p21 induction, 50 nM FP caused G_1 and G_2 arrest, measured by flow cytometry (Fig. 2B). In agreement, 50 nM inhibited incorporation of [^3H]thymidine (Fig. 2C); 50 nM FP only slightly affected cell survival at day 3, as evaluated by MTT (Fig. 2C). Thus, cytostatic concentrations of FP paradoxically induce p21 instead of p53. For comparison, p53-inducing concentrations of FP completely inhibited cell survival by 3 days of treatment (Fig. 2C; 500 nM).

Superinduction of p53-Dependent Transcription by Removing FP. Thus, low concentrations (50–60 nM) of FP caused induction of p21 in LNCaP cells (Fig. 2A and Fig. 3A). If induction of p21 is caused by spontaneous resumption of transcription, then such an induction can be reproduced at high concentrations (400–500 nM) by a mere change of the medium. Change of the medium resulted in superinduction of p21 and Mdm-2 (superinduction).

As expected, 400 nM FP induced p53 but not p21 and Mdm-2. After the medium was changed (release), Mdm-2 and p21 were induced dramatically (Fig. 3A; FP 400, release). Thus, the inhibition of Mdm-2 and p21 was reversible, as evidenced by rebound of Mdm-2 and p21. Therefore, we expected that restoration of transcription would reverse the cytotoxicity. We incubated LNCaP cells with FP for either 3 days or 16 h (and then incubated in the fresh medium). Four hundred nM FP maximally inhibited cell viability (Fig. 3B). When FP was washed out after 16 h, the effect was reversed. The cytotoxicity of pulse treatment with 400 nM FP and continual treatment with 60 nM FP were similar (Fig. 3B, arrows), corresponding to rebound of p21.

Similarly, DRB, an inhibitor of transcription, induced wild-type p53 with only minimal induction of p21 and Mdm-2 (34). Change of the medium (release) resulted in superinduction of Mdm-2 and p21, decreasing p53 levels (34). Thus, effects of two inhibitors of transcription (FP and DRB) were identical (34).

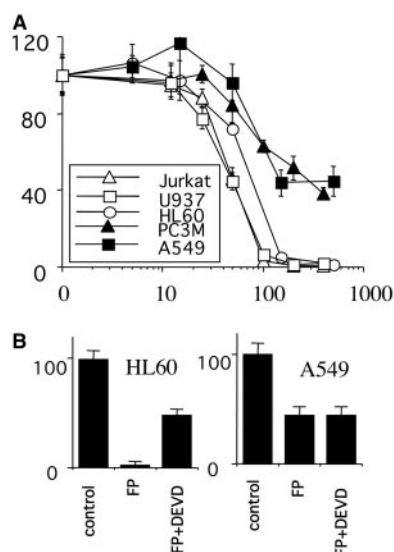
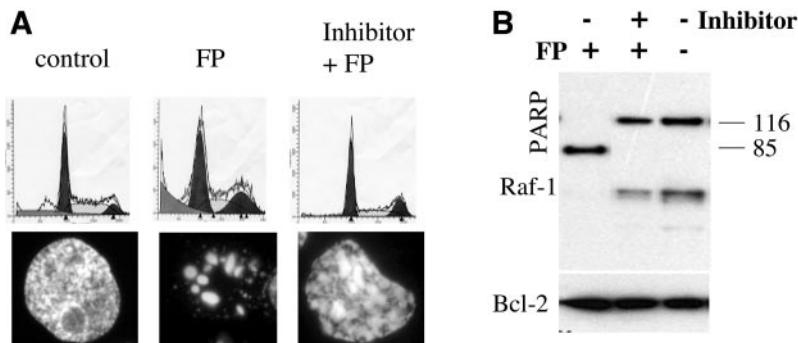


Fig. 4. Cytotoxicity of flavopiridol (FP): two types of cell lines. **A**, Jurkat, U937, and HL60 (apoptosis-prone) leukemia cell lines and PC3M and A549 (apoptosis-resistant) cancer cell lines were treated with FP for 3 days, and MTT assay was performed as described in "Materials and Methods." **B**, HL60 and A549 cells were treated either with FP (300 nM) or with FP plus 20 μM z-DEVD-fmk for 48 h, and MTT assay was performed as described in "Materials and Methods."

Fig. 5. Flavopiridol (FP)-induced apoptosis in HL60 cells. A, effects of caspase inhibitors on nuclear fragmentation (top) and cell cycle distribution (bottom). HL60 cells were treated for 16 h with either 300 nM FP or 300 nM FP plus 20 μ M caspase inhibitor (*Inhibitor + FP*): z-DEVD-fmk [bottom, 4',6-diaminidino-2-phenylindole (DAPI)] and B-d-fmk (top, flow cytometry). DAPI staining and flow cytometry were performed as described in "Materials and Methods." B, effects of caspase inhibitors on poly(ADP-ribose) polymerase (PARP) and Raf-1 cleavage. HL60 cells were treated with FP and FP plus 20 μ M z-DEVD-fmk (*FP + Inhibitor*) for 16 h. Immunoblot analysis for PARP, Raf-1, and Bcl-2 (for equal loading) was performed as described in "Materials and Methods."



We next investigated superinduction of p53-dependent transcription using a p53-responsive reporter plasmid, PG13-Luc, whose promoter contains 13 p53 binding sites. We transfected cells with either PG13-Luc or pGL2-Luc (a p53-independent promoter-Luc construct) and then treated cells with FP. As expected, in the presence of transcriptional inhibitors, PG13-Luc and pGL2-Luc were inhibited (Fig. 3C). Once FP was removed, PG13-Luc was superinduced, whereas pGL2-Luc was not.

We next investigated the superinduction of Mdm-2 (after removal of FP) and its effect on p53. In A549 cells, high concentrations of FP dramatically induced p53 but inhibited Mdm-2. Change of the medium resulted in induction of Mdm-2 by 12 h. Induction of Mdm-2 was followed by decrease of p53 to its basal levels (Fig. 3D).

Apoptosis-Prone and -Reluctant Cell Lines. Although induction of p53 and cytotoxicity correlated (in cells with wild-type p53), this correlation does not necessarily mean that p53 causes cytotoxic effects. Up-regulation of p53 may be a mere marker of effective concentrations of FP. We compared effects of FP on leukemia cell lines HL60, Jurkat, and U937, which generally are sensitive to most anti-cancer drugs, and on A549 and PC3M cancer cell lines. Two types of cell lines could be easily distinguished by a simple MTT assay (Fig. 4A). At concentrations ≥ 100 nM, FP completely inhibited survival of leukemia cell lines (MTT values approached zero, indicating absence of live cells that are able to metabolize MTT). Cell death was confirmed by loss of trypan blue exclusion. In A549 and PC3M cells, MTT values were not decreased $<40\%$ of control (Fig. 4A), and these cells remained attached to the plastic and excluded trypan blue (data not shown).

We next investigated effects of the inhibitor of caspases, z-DEVD-fmk, in HL60 and A549 cells (Fig. 4B). z-DEVD-fmk protected HL60

cells from FP. z-DEVD had no effect on A549 cells, which were, to start with, refractory to FP. In the presence of z-DEVD-fmk, HL60 cells were as refractory as A549 cells (Fig. 4B).

Effects in Apoptosis-Prone Cells. In agreement with caspase inhibitor-dependent effects (Fig. 4B; HL60), FP caused massive apoptosis in these leukemia cells (Fig. 5). FP caused nuclear fragmentation (visualized by DAPI staining) and DNA fragmentation (sub-G₁ DNA content), measured by flow cytometry (Fig. 5A) and PARP and Raf-1 cleavage (Fig. 5B). Inhibitors of caspases, z-DEVD-fmk and BD-fmk, prevented apoptosis: nuclear fragmentation and sub-G₁ peak (Fig. 5A). They also blocked PARP and Raf-1 cleavage. Noteworthy, in these apoptosis-prone cells, FP depleted caspase-cleaved proteins (e.g., Raf-1 and PARP), and caspase inhibitors can restore the expression of such proteins. While preventing apoptosis, caspase inhibitors unmasked growth arrest. Literally, caspase inhibitors transformed apoptosis to growth arrest (Fig. 5A).

FP Potentiates Apoptosis in A549 Cells. In A549 cells, FP induced p53, as a marker of global inhibition of transcription. It is known that inhibitors of transcription sensitize cells to TNF. This predicts that p53 induction should correlate with cell sensitization to TNF. We confirmed this prediction (Fig. 6). Neither FP nor TNF caused apoptosis in A549 cells (Fig. 6A). Added together, FP and TNF caused rapid and massive apoptosis (Fig. 6A). In 12–16 h, 50% of cells showed nuclear fragmentation (Fig. 6A). One hundred nM and 400 nM FP exerted comparable short-term effects (16 h), such as potentiation of TNF-induced apoptosis (Fig. 6A) and induction of p53 (Fig. 6B). Please note that 100 nM FP alone was only minimally cytotoxic in long-term assay (Fig. 4A), indicating a transient effect of low concentrations of FP. However, even transient effects of FP were

Fig. 6. Apoptosis caused by a combination of tumor necrosis factor (TNF) and flavopiridol (FP) in A549 cells. A, A549 cells were treated with 100 nM or 400 nM FP without (–TNF) or with 5 ng/ml TNF (+TNF). 4',6-Diaminidino-2-phenylindole staining was performed after 12 h. B, A549 cells were treated with 100 nM or 400 nM FP without (–TNF) or with 5 ng/ml TNF (+TNF). Immunoblot analysis for Hsp90 and p53 was performed as described in "Materials and Methods." C, A549 cells were treated with FP (400 nM), TNF (5 ng/ml), FP + TNF (cells treated with FP and then TNF was added after 2 and 5 h as indicated), TNF + FP (cells treated with TNF and then FP was added after 2 and 5 h as indicated), TNF and FP were added together (0 h). MTT assay was performed after 36 h.

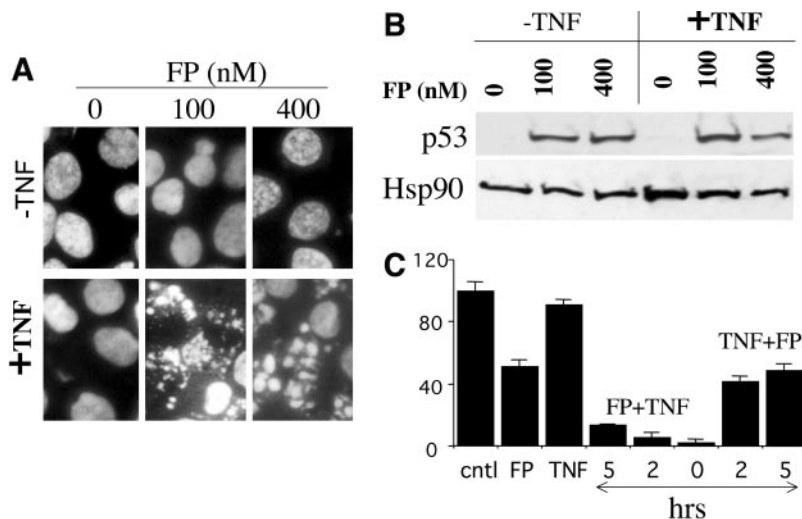
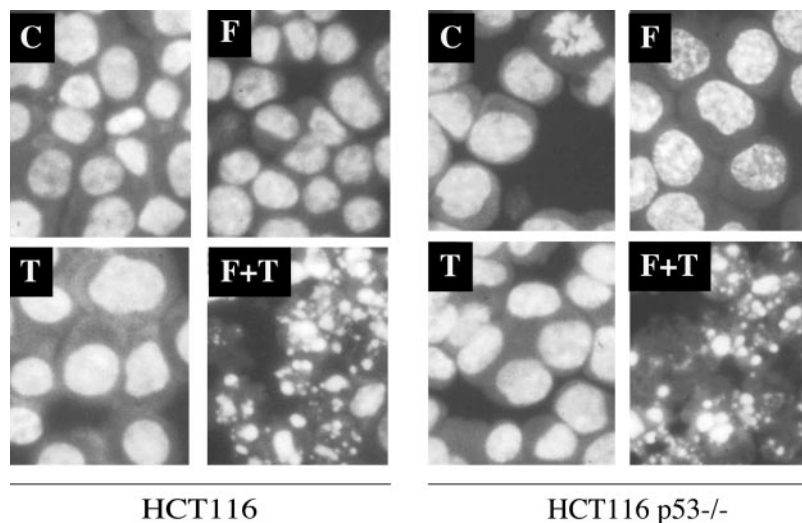


Fig. 7. Tumor necrosis factor (*TNF*) and flavopiridol (*FP*) cause apoptosis independent of p53. HCT116 cells and HCT116 p53^{-/-} cells were treated with 400 nM FP (*F*), 5 ng/ml TNF (*T*), FP + TNF (*F + T*), or left untreated (*c*). 4',6-Diamidino-2-phenylindole staining was performed after 16 h.



sufficient to cause permanent effect (apoptosis) when these transiently “sensitized” cells were treated with TNF (Fig. 6A).

The most significant cytotoxicity was observed when FP and TNF were added together (Fig. 6C). When FP was added before TNF, the cytotoxicity was slightly decreased, although it still was prominent. However, when TNF was added before FP, no synergy was observed (Fig. 6C). This also was confirmed by DAPI staining and microscopy (data not shown). TNF induces antiapoptotic proteins, which in turn antagonize activation of caspases (39, 40). By inhibiting transcription, FP then allowed TNF to induce apoptosis. For example, TNF increased Hsp90 (an antiapoptotic protein), and this induction was blunted by FP (Fig. 6B). Thus, induction of p53 coincided with sensitization to TNF-induced apoptosis. We next take advantage of two isogenic cell lines that differ in p53 status: parental HCT116 colon cancer cells and HCT116 p53^{-/-}, p53 knockout HCT116 cells. Neither FP nor TNF alone induced apoptosis in these cells after 16 h of treatment (Fig. 7). Added together, FP and TNF caused nuclear fragmentation in parental and p53^{-/-} cells (Fig. 7). This suggests that induction of p53 is not required for FP-induced sensitization to TNF.

FP Potentiates TNF in PC3M Cells. We next investigated a combination of FP and TNF in PC3M cells, which lack p53. TNF alone had no measurable effect on proliferation and survival of PC3M cells (Fig. 8). FP inhibited proliferation of PC3M cells by causing G₁ arrest (Fig. 8A). When PC3M cells were cotreated with FP and TNF, growth arrest was transformed to apoptosis, as evidenced by sub-G₁ peak (Fig. 8A) and caspase-8 and -9 cleavage (Fig. 8B). This was followed by cessation of metabolism (a hallmark of cell death), as evidenced by the decrease in MTT metabolism (Fig. 8C). It is important that the synergy between FP and TNF was sequence dependent. Thus, pretreatment with FP rendered PC3M sensitive to TNF, whereas pretreatment with TNF did not (Fig. 8C). It is noteworthy that pretreatment with FP was as effective as simultaneous administration of FP and TNF (Fig. 8C).

In the presence of TNF, FP was as cytotoxic to PC3M as FP alone was cytotoxic to U937: respective cytotoxicity curves were lined up (Fig. 9A).

To start with, U937 cells were sensitive to TNF and FP (Fig. 9B). However, when combined, FP and TNF potentiated one another (Fig. 9B). This potentiation occurred at narrow concentrations (50 nM) of FP. At higher concentrations, FP alone was cytotoxic to U937 cells (Fig. 9C, *insert*). Therefore, potentiation by TNF was observed mainly at suboptimal concentrations of FP. Furthermore, this potentiation was sequence independent (Fig. 9B). Addition of TNF simultaneously with FP or before or after FP was equally effective (Fig. 9B). Thus, in

U937 cells, each agent alone can cause apoptosis, potentiating each other in a sequence-independent manner. In apoptosis-reluctant PC3M and A549 cells, neither agent alone caused apoptosis. In these cells, apoptotic combinations of FP and TNF were strictly sequence dependent.

DISCUSSION

Normally, wild-type p53 transcriptionally induces Mdm-2 and p21 (Fig. 10A). In turn, Mdm-2 binds p53 and targets it for degradation. In addition to Mdm-2, p21 also is required for efficient p53 degradation at least in certain cell lines (34). DNA-damaging drugs induce p53, which in turn induces p21 and Mdm-2 (41). We showed that, although inducing p53, FP inhibited p21 and Mdm-2. Similar results were obtained with all of the inhibitors of transcription (actinomycin D, amanitin, and DRB; Refs. 34, 42) and FP (herein). We can conclude that up-regulation of p53 accompanied by down-regulation of p21/

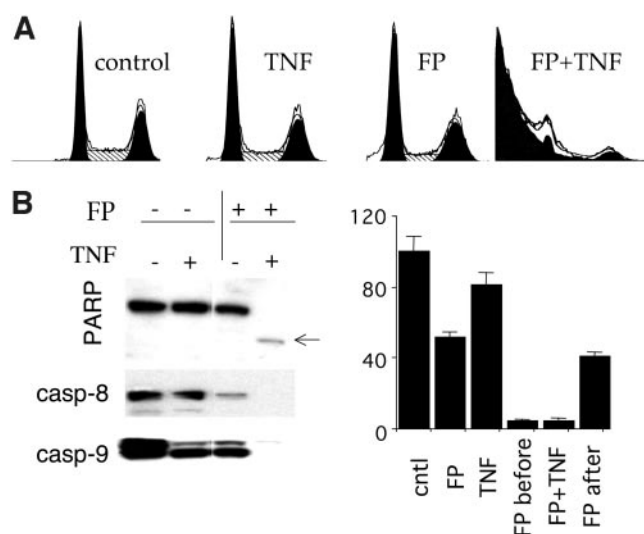


Fig. 8. Potentiation of tumor necrosis factor (*TNF*) by flavopiridol (*FP*) in p53-null PC3M cells. *A* and *B*, PC3M cells were treated with 500 nM FP and 5 ng/ml TNF overnight as indicated. *A*, flow cytometry. *B*, immunoblot for poly(ADP-ribose) polymerase (*PARP*) and caspase-8, and -9. *C*, PC3M cells were treated with FP (400 nM) or TNF (5 ng/ml); cells were treated with FP, and TNF was added after 5 h (*FP before*); TNF and FP were added together (*FP + TNF*); or cells were treated with TNF, and FP was added after 5 h (*FP after*). MTT assay was performed after 36 h.

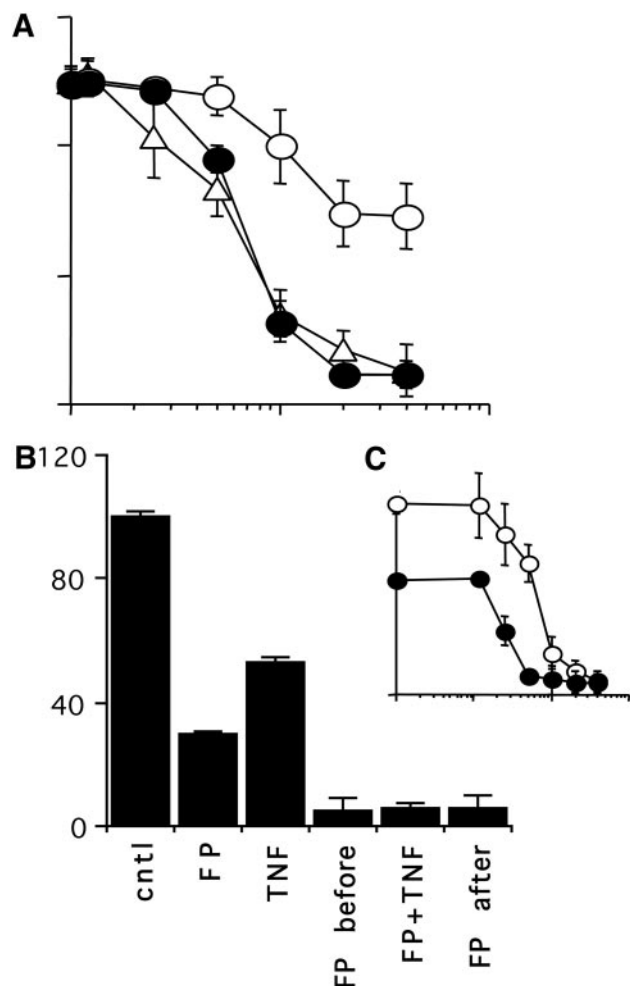


Fig. 9. Effects of transcriptional inhibitors on flavopiridol (FP)-induced cytotoxicity in PC3M and U937 cells. *A*, cells were treated with indicated concentrations of FP (X axis) with or without 5 ng/ml tumor necrosis factor (*TNF*) as shown: PC3M treated with FP alone (○); PC3M cotreated with FP + *TNF* (●); or U937 treated with FP alone (△). MTT assay was performed after 3 days as described in "Materials and Methods." *B*, U937 cells were treated with FP (50 nM) or *TNF* (5 ng/ml); cells were treated with FP, and *TNF* was added after 5 h (*FP before*); *TNF* and FP were added together (*FP + TNF*); or cells were treated with *TNF*, and FP was added after 5 h (*FP after*). MTT assay was performed after 36 h. *C, insert*, U937 cells were treated with indicated concentrations of FP (X axis) with (○) or without 5 ng/ml *TNF* (●). MTT assay was performed as described in "Materials and Methods."

Mdm-2 is a characteristic hallmark of inhibition of transcription (Fig. 10B). Transcription could be restored either by removal of FP or spontaneously (at low concentrations of FP). In the presence of induced p53, removal of FP resulted in superinduction of a p53-dependent transcription, measured by the p53-dependent reporter construct PG13-Luc. This was accompanied by induction of p21 and Mdm-2. Induction of p21 by low concentrations of FP can be driven by the accumulated p53. Although some cells may resume transcription (high p21), some cells still have transcription shut down (high p53). Total cell population includes cells with low p21 and high p53 (Fig. 10B) and cells with high p21 and low p53 (Fig. 10C). This explains why low concentrations of FP can increase p53 and p21, as measured by immunoblot analysis.

Whereas low concentrations of FP cause transient effects and induction of p21, higher concentrations sustained lasting low levels of p21 and Mdm-2 accompanied by dramatic accumulation of p53. Accumulation of p53, in turn, correlates with maximal cytotoxic effects of FP. Concentrations of FP >100–200 nM induced p53 and caused maximal cytotoxicity. However, p53 was a marker, not a

cause, of cytotoxicity. In cells lacking p53, FP was maximally cytotoxic at the same concentrations (>100 nM). Furthermore, at concentrations that induce p53 in cells with wild-type p53, FP caused rapid apoptosis in p53-deficient cells (Jurkat, U937, and HL60). In agreement with previous reports, p53 was dispensable for FP-induced apoptosis (23, 33, 43). It has been shown that 100–500 nM FP caused either cell cycle arrest or apoptosis (7, 23, 44, 45). Apoptosis is a desirable mechanism of drug-induced cell death (46). What determines a choice between apoptosis and cycle arrest? FP induced apoptosis in Jurkat, HL60, and U937 cells but inhibited proliferation in PC3M and A549 cells. In HL60, Jurkat, and U937 cells, anticancer drugs, including doxorubicin, paclitaxel, inhibitors of proteasome, and inhibitors of HDAC, induce apoptosis, cell death mediated by caspases. Likewise, FP induced apoptosis in these cell lines. When apoptosis was blocked by inhibitors of caspases (z-DEVD-fmk and BD-fmk), HL60 cells underwent growth arrest (Fig. 11). In apoptosis-reluctant cells, such as A549 and PC3M, FP induced growth arrest. In these cells, most anticancer drugs also do not induce apoptosis (47). In summary, FP induces (a) apoptosis and growth arrest, masked by apoptosis, in cells with intact apoptotic pathways (HL60, Jurkat, and U937) and (b) growth arrest in cells with inhibited apoptotic pathways (A549

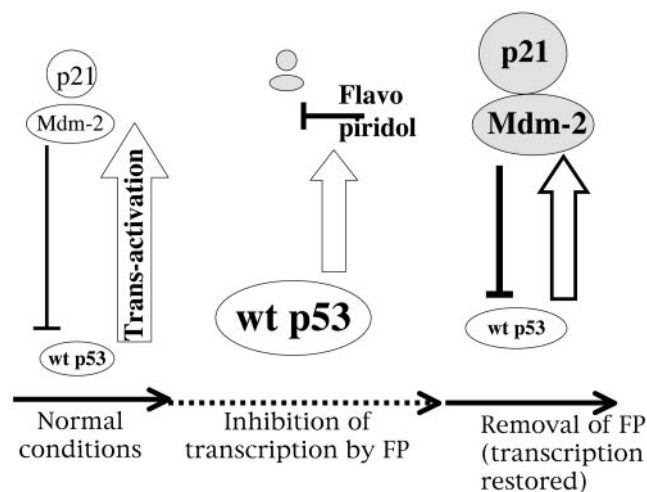


Fig. 10. Mechanisms of p53, p21, and Mdm-2 inductions following transient treatment with flavopiridol (FP). *A*, normal conditions. p53 transcriptionally induces Mdm-2, which targets p53 for degradation. *B*, inhibition of transcription. p53 cannot induce Mdm-2. In the absence of Mdm-2, p53 cannot be degraded, and p53 accumulates. *C*, removal of flavopiridol. p53 that is highly overexpressed strongly induced Mdm-2 and p21. Highly overexpressed Mdm-2 decreases levels of p53.

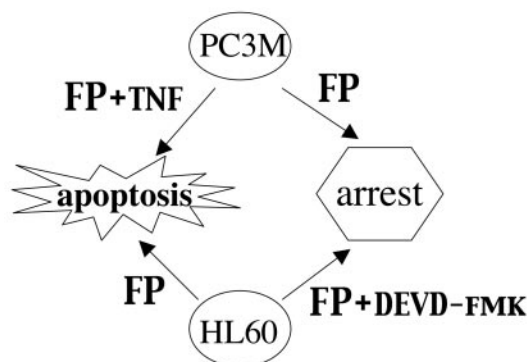


Fig. 11. Conversion of flavopiridol (FP)-induced apoptosis to cycle arrest and vice versa. In apoptosis-reluctant PC3M cells, FP causes cell cycle arrest. Addition of tumor necrosis factor (*FP + TNF*) causes apoptosis. In apoptosis-prone HL60 cells, FP causes apoptosis. Addition of the caspase inhibitor z-DEVD-fmk unmasks cell cycle arrest.

and PC3M). In HL60 cells, inhibition of caspases transforms apoptosis to growth arrest and slow nonapoptotic death. In A549 and PC3M cells, apoptotic pathways are intrinsically inhibited, and these cells undergo cell cycle arrest and slow cell death. By decreasing inhibitors of apoptosis proteins and other short-lived antiapoptotic proteins, inhibitors of transcription can deblock apoptotic pathways. Actinomycin D can render cells sensitive to TNF. Similarly, TNF plus FP caused apoptosis in A549 and PC3M cells. TNF activates the extrinsic caspase cascade and transcriptionally induces antiapoptotic proteins, such as inhibitors of apoptosis proteins, RIP, and FLIP (48). Similarly, we demonstrated here that FP must be added simultaneously or before TNF to sensitize cells to TNF-induced apoptosis. In contrast, in apoptosis-prone U937 cells (cells with intact apoptotic pathways), TNF and FP potentiated each other in a sequence-independent fashion. While our manuscript was in preparation, it has been shown that FP blocked NF κ B, thus sensitizing cancer cells to TNF (49). We suggest that sensitization to TNF-induced apoptosis is caused by universal inhibition of transcription. In addition to NF κ B, other pathways also induce antiapoptotic proteins (48). FP (because of its global inhibition of transcription) inhibits any antiapoptotic proteins that have a short-lived expression. Universal inhibition of transcription by FP can cause its cytotoxicity and explains a variety of results reported in the literature. For example, FP disrupts sodium butyrate-induced p21 expression and differentiation (16, 50). Both p21 induction and differentiation are transcriptional processes and must be prevented by FP. In addition to the primary inhibition of transcription, leading to disappearance of short-lived RNAs and proteins, FP secondarily depletes caspase-cleaved proteins in apoptosis-prone cells. For example, PARP and Raf-1 were cleaved during FP-induced apoptosis in HL60 cells (Fig. 5D). Caspase inhibitors restored expression of these proteins. Recognition of this double mechanism of protein depletion (in apoptosis-prone cells only) can sort out an enormous complexity in the literature. For example, p21 may be down-regulated by both mechanisms: transcriptional inhibition (in all of the cells) and cleavage by caspase (in cells that undergo apoptosis). Finally, other inhibitors of kinases may inhibit transcription. In this light, it is interesting that butyrolactone also down-regulates p21, whereas it induces p53 (51). As another example, bisindolylmaleimide IX, initially described as an inhibitor of protein kinase C, inhibits transcription and sensitized cells to TNF and TNF-related apoptosis-inducing ligand (52). Intriguingly, the protein kinase C δ inhibitor rottlerin affects mitochondrial function independent of protein kinase C δ , sensitizing cells to TNF-related apoptosis-inducing ligand (53).

Thus far, FP has not demonstrated activity as a single agent in patients with advanced colorectal cancer (54), metastatic renal cancer (5), and metastatic prostate cancer (55). However, FP may have tremendous clinical potential if used as an inhibitor of transcription in mechanism-based drug combinations. One approach is to combine FP with proapoptotic and differentiating agents (TNF-related apoptosis-inducing ligand and phorbol ester) to induce apoptosis in resistant cancers. FP also can prevent a protective transcriptional response caused by certain anticancer drugs. This explains augmentation by FP of apoptosis and tumor regression caused by CPT-11 (3), paclitaxel (56), and radiation (10).

Although actinomycin D (dactinomycin) has been used in cancer therapy for >40 years, at clinically relevant cytotoxic concentrations, it is a DNA-damaging drug rather than an inhibitor of transcription (57). For FP, cytotoxic concentrations and therapeutic doses coincide with those that ascribed to inhibition of transcription. With this in mind, FP may be the first inhibitor of transcription that is used clinically. Because of such an explicit and unique mechanism of action, it may have numerous clinical applications in drug combinations.

ACKNOWLEDGMENTS

We thank Robert Robey (NCI, NIH) for his help in performing flow cytometry.

REFERENCES

- Arguello F, Alexander M, Sterry JA, et al. Flavopiridol induces apoptosis of normal lymphoid cells, causes immunosuppression, and has potent antitumor activity in vivo against human leukemia and lymphoma xenografts. *Blood* 1998;91:2482–90.
- Patel V, Senderowicz AM, Pinto DJ, et al. Flavopiridol, a novel cyclin-dependent kinase inhibitor, suppresses the growth of head and neck squamous cell carcinomas by inducing apoptosis. *J Clin Invest* 1998;102:1674–81.
- Motwani M, Jung C, Sirotak FM, et al. Augmentation of apoptosis and tumor regression by flavopiridol in the presence of CPT-11 in Hct116 colon cancer monolayers and xenografts. *Clin Cancer Res* 2001;7:4209–19.
- Newcomb EW, Tamasdan C, Entzminger Y, et al. Flavopiridol inhibits the growth of GL261 gliomas in vivo: implications for malignant glioma therapy. *Cell Cycle* 2004;3:230–4.
- Stadler WM, Vogelzang NJ, Amato R, et al. Flavopiridol, a novel cyclin-dependent kinase inhibitor, in metastatic renal cancer: a University of Chicago Phase II Consortium study. *J Clin Oncol* 2000;18:371–5.
- Thomas JP, Tutsch KD, Cleary JF, et al. Phase I clinical and pharmacokinetic trial of the cyclin-dependent kinase inhibitor flavopiridol. *Cancer Chemother Pharmacol* 2002;50:465–72.
- Schwartz GK, O'Reilly E, Ilson D, et al. Phase I study of the cyclin-dependent kinase inhibitor flavopiridol in combination with paclitaxel in patients with advanced solid tumors. *J Clin Oncol* 2002;20:2157–70.
- Senderowicz AM. Novel small molecule cyclin-dependent kinases modulators in human clinical trials. *Cancer Biol Ther* 2003;2:S84–95.
- Carlson BA, Dubay MM, Sausville EA, Brizuela L, Worland PJ. Flavopiridol induces G1 arrest with inhibition of cyclin-dependent kinase (CDK) 2 and CDK 4 in human breast carcinoma cells. *Cancer Res* 1996;56:2973–8.
- Raju U, Nakata E, Mason KA, Ang KK, Milas L. Flavopiridol, a cyclin-dependent kinase inhibitor, enhances radiosensitivity of ovarian carcinoma cells. *Cancer Res* 2003;63:3263–7.
- Rane SG, Dubus P, Mettus RV, et al. Loss of Cdk4 expression causes insulin-deficient diabetes and Cdk4 activation results in β -islet cell hyperplasia. *Nat Genet* 1999;22:44–52.
- Tetsu O, McCormick F. Proliferation of cancer cells despite cdk2 inhibition. *Cancer Cell* 2003;3:233–45.
- Ortega S, Prieto I, Odajima J, et al. Cyclin-dependent kinase 2 is essential for meiosis but not for mitotic cell division in mice. *Nat Genet* 2003;35:25–31.
- Aleem E, Berthet C, Kaldis P. Cdk2 as a master of S phase entry: fact or fake? *Cell Cycle* 2004;3:35–7.
- Bible KC, Kaufmann SH. Flavopiridol: a cytotoxic flavone that induces cell death in noncycling A549 human lung carcinoma cells. *Cancer Res* 1996;56:4856–61.
- Rosato RR, Almenara JA, Cartee L, Betts V, Chellappan SP, Grant S. The cyclin-dependent kinase inhibitor flavopiridol disrupts sodium butyrate-induced p21WAF1/CIP1 expression and maturation while reciprocally potentiating apoptosis in human leukemia cells. *Mol Cancer Ther* 2002;1:253–66.
- Gojo I, Zhang B, Fenton R. The cyclin-dependent kinase inhibitor flavopiridol induces apoptosis in multiple myeloma cells through transcriptional repression and down-regulation of Mcl-1. *Clin Cancer Res* 2002;8:3527–38.
- Ma Y, Cress WD, Haura EB. Flavopiridol-induced apoptosis is mediated through up-regulation of E2F1 and repression of Mcl-1. *Mol Cancer Ther* 2003;2:73–81.
- Carlson B, Lahusen T, Singh S, et al. Downregulation of cyclin D1 by transcriptional repression in MCF-7 human breast carcinoma cells induced by flavopiridol. *Cancer Res* 1999;59:4634–41.
- Melillo G, Sausville EA, Cloud K, Lahusen T, Varesio L, Senderowicz AM. Flavopiridol, a protein kinase inhibitor, down-regulates hypoxic induction of vascular endothelial growth factor expression in human monocytes. *Cancer Res* 1999;59:5433–7.
- Kitada S, Zapata J, Andreeff M, Reed JC. Protein kinase inhibitors flavopiridol and 7-hydroxy-staurosporine down-regulate antiapoptosis proteins in B-cell chronic lymphocytic leukemia. *Blood* 2000;96:393–7.
- Wittmann S, Bali P, Donapaty S, et al. Flavopiridol down-regulates antiapoptotic proteins and sensitizes human breast cancer cells to epothilone B-induced apoptosis. *Cancer Res* 2003;63:93–9.
- Shapiro GI, Koestner DA, Matranga CB, Rollins BJ. Flavopiridol induces cell cycle arrest and p53-independent apoptosis in non-small cell lung cancer cell lines. *Clin Cancer Res* 1999;5:2925–38.
- Bible KC, Bible RHJ, Kottke TJ, et al. Flavopiridol binds to duplex DNA. *Cancer Res* 2000;60:2419–28.
- Peng J, Zhu Y, Milton JT, Price DH. Identification of multiple cyclin subunits of human P-TEFb. *Genes Dev* 1998;12:755–62.
- Chao SH, Price DH. Flavopiridol inactivates P-TEFb and blocks most RNA polymerase II transcription in vivo. *J Biol Chem* 2001;276:31793–9.
- Lam LT, Pickeral OK, Peng AC, et al. Genomic-scale measurement of mRNA turnover and the mechanisms of action of the anti-cancer drug flavopiridol. *Genome Biol* 2001;0041.
- Ni Z, Schwartz BE, Werner J, Suarez JR, Lis JT. Coordination of transcription, RNA processing, and surveillance by P-TEFb kinase on heat shock genes. *Mol Cell* 2004;13:55–65.

29. de Azevedo WFJ, Canduri F, da Silveira NJ. Structural basis for inhibition of cyclin-dependent kinase 9 by flavopiridol. *Biochem Biophys Res Commun* 2002;293:566–71.
30. Price DH. P-TEFb, a cyclin-dependent kinase controlling elongation by RNA polymerase II. *Mol Cell Biol* 2000;20:2629–34.
31. Poele RHT, Okorokov AL, Joel SP. RNA synthesis block by 5,6-dichloro-1- β -D-ribofuranosylbenzimidazole (DRB) triggers p53-dependent apoptosis in human colon carcinoma cells. *Oncogene* 1999;18:5765–72.
32. Nahta R, Trent S, Yang C, Schmidt EV. Epidermal growth factor receptor expression is a candidate target of the synergistic combination of trastuzumab and flavopiridol in breast cancer. *Cancer Res* 2003;63:3626–31.
33. Alonso M, Tamasdan C, Miller DC, Newcomb EW. Flavopiridol induces apoptosis in glioma cell lines independent of retinoblastoma and p53 tumor suppressor pathway alterations by a caspase-independent pathway. *Mol Cancer Ther* 2003;2:139–50.
34. Blagosklonny MV, Demidenko ZN, Fojo T. Inhibition of transcription results in accumulation of Wt p53 followed by delayed outburst of p53-inducible proteins: p53 as a sensor of transcriptional integrity. *Cell Cycle* 2002;1:67–74.
35. Konig A, Schwartz GK, Mohammad RM, Al-Katib A, Gabrilove JL. The novel cyclin-dependent kinase inhibitor flavopiridol downregulates Bcl-2 and induces growth arrest and apoptosis in chronic B-cell leukemia lines. *Blood* 1997;90:4307–12.
36. Blagosklonny MV, Giannakakou P, Romanova LY, Ryan KM, Vousden KH, Fojo T. Inhibition of HIF-1- and wild-type p53-stimulated transcription by codon Arg175 p53 mutants with selective loss of functions. *Carcinogenesis* 2001;22:861–7.
37. Inga A, Storicci F, Darden T, Resnick M. Differential transactivation by the p53 transcription factor is highly dependent on p53 level and promoter target sequence. *Mol Cell Biol* 2002;22:8612–25.
38. Bar-Or RL, Maya R, Segel LA, Alon U, Levine AJ, Oren M. Generation of oscillations by the p53-mdm2 feedback loop: a theoretical and experimental study. *Proc Natl Acad Sci USA* 2000;97:11250–5.
39. Wang CY, Mayo MW, Korneluk RG, Goeddel DV, Baldwin ASJ. NF- κ B antiapoptosis: induction of TRAF1 and TRAF2 and c-IAP1 and c-IAP2 to suppress caspase-8 activation. *Science* 1998;281:1680–3.
40. Natoli G, Costanzo A, Guido F, et al. Nuclear factor κ B-independent cytoprotective pathways originating at tumor necrosis factor receptor-associated factor 2. *J Biol Chem* 1998;273:31262–72.
41. Hayon IL, Haupt Y. p53: an internal investigation. *Cell Cycle* 2002;1:111–6.
42. An WG, Hwang SG, Trepel JB, Blagosklonny MV. Protease inhibitor-induced apoptosis: accumulation wt p53, p21WAF1/CIP1, and induction of apoptosis are independent markers of proteasome inhibition. *Leukemia* 2000;14:1276–83.
43. Pepper C, Thomas A, Hoy T, et al. Leukemic and non-leukemic lymphocytes from patients with Li Fraumeni syndrome demonstrate loss of p53 function, Bcl-2 family dysregulation and intrinsic resistance to conventional chemotherapeutic drugs but not flavopiridol. *Cell Cycle* 2003;2:53–8.
44. Parker BW, Kaur G, Nieves-Neira W, et al. Early induction of apoptosis in hematopoietic cell lines after exposure to flavopiridol. *Blood* 1998;91:458–65.
45. Schwartz GK. CDK inhibitors: cell cycle arrest versus apoptosis. *Cell Cycle* 2002;1:122–3.
46. Houghton JA. Apoptosis and drug response. *Curr Opin Oncol* 1999;11:475–81.
47. Zhitovitsky B, Orrenius S. Defects in the apoptotic machinery of cancer cells: role in drug resistance. *Semin Cancer Biol* 2003;13:125–34.
48. Kim Y, Suh N, Sporn M, Reed JC. An inducible pathway for degradation of FLIP protein sensitizes tumor cells to TRAIL-induced apoptosis. *J Biol Chem* 2002;277:22320–9.
49. Kim D, Koo SY, Jeon K, et al. Rapid induction of apoptosis by combination of flavopiridol and tumor necrosis factor (TNF)- α or TNF-related apoptosis-inducing ligand in human cancer cell lines. *Cancer Res* 2003;63:621–6.
50. Cartee L, Wang Z, Decker RH, et al. The cyclin-dependent kinase inhibitor (CDKI) flavopiridol disrupts phorbol 12-myristate 13-acetate-induced differentiation and CDKI expression while enhancing apoptosis in human myeloid leukemia cells. *Cancer Res* 2001;61:2583–91.
51. Sax JK, Dash BC, Hong R, Dicker DT, El-Deiry WS. The cyclin-dependent kinase inhibitor butyrolactone is a potent inhibitor of p21WAF1/CIP1 expression. *Cell Cycle* 2002;1:90–6.
52. Rokhlin OW, Cohen MB. Bisindolylmaleimide IX induces reversible and time-dependent tumor necrosis factor receptor family-mediated caspase activation and cell death. *Cancer Biol Ther* 2003;2:266–70.
53. Tillman DM, Izeradjene K, Szucs KS, Douglas L, Houghton JA. Rottlerin sensitizes colon carcinoma cells to tumor necrosis factor-related apoptosis-inducing ligand-induced apoptosis via uncoupling of the mitochondria independent of protein kinase C. *Cancer Res* 2003;63:5118–25.
54. Aklilu M, Kindler HL, Donehower RC, Mani S, Vokes EE. Phase II study of flavopiridol in patients with advanced colorectal cancer. *Ann Oncol* 2003;14:1270–3.
55. Liu G, Gandara DR, Lara PNJ, et al. A phase II trial of flavopiridol (NSC #649890) in patients with previously untreated metastatic androgen-independent prostate cancer. *Clin Cancer Res* 2004;10:924–8.
56. Motwani M, Delohery TM, Schwartz GK. Sequential dependent enhancement of caspase activation and apoptosis by flavopiridol on paclitaxel-treated human gastric and breast cancer cells. *Clin Cancer Res* 1999;5:1876–83.
57. Osathanondh R, Goldstein DP, Pastoride GB. Actinomycin D as the primary agent for gestational trophoblastic disease. *Cancer* 1975;36:863–6.

Cancer Research

The Journal of Cancer Research (1916–1930) | The American Journal of Cancer (1931–1940)

Flavopiridol Induces p53 via Initial Inhibition of Mdm2 and p21 and, Independently of p53, Sensitizes Apoptosis-Reluctant Cells to Tumor Necrosis Factor

Zoya N. Demidenko and Mikhail V. Blagosklonny

Cancer Res 2004;64:3653-3660.

Updated version Access the most recent version of this article at:
<http://cancerres.aacrjournals.org/content/64/10/3653>

Cited articles This article cites 56 articles, 33 of which you can access for free at:
<http://cancerres.aacrjournals.org/content/64/10/3653.full#ref-list-1>

Citing articles This article has been cited by 12 HighWire-hosted articles. Access the articles at:
<http://cancerres.aacrjournals.org/content/64/10/3653.full#related-urls>

E-mail alerts [Sign up to receive free email-alerts](#) related to this article or journal.

Reprints and Subscriptions To order reprints of this article or to subscribe to the journal, contact the AACR Publications Department at pubs@aacr.org.

Permissions To request permission to re-use all or part of this article, contact the AACR Publications Department at permissions@aacr.org.